5

Graphene Synthesis, Catalysis with Transition Metals and Their Interactions by Laser Photolysis

Bonex W Mwakikunga[1,2] and Kenneth T Hillie[1,3]
[1]*Council for Scientific and Industrial Research, National Centre for Nano-structured Materials, Pretoria*
[2]*Department of Physics and Biochemical Sciences, University of Malawi, The Malawi Polytechnic, Chichiri, Blantyre,*
[3]*Department of Physics, University of Free State, Bloemfontein,*
[1,3]*South Africa*
[2]*Malawi*

1. Introduction

This chapter introduces some facts about graphene, how it was discovered, how it has been realised by several approaches and how to get its identity. Its identity is seen either through cross-sectional TEM or through its unique signature in Raman spectra. We also briefly review bottom-up and top-down synthesis approaches that have led either to few layers or monolayer graphene. We discuss the photochemical mechanisms and process of the formation of graphene, graphene's catalysis of the vanadium oxide mono-layers, the defects leading to inorganic fullerenes of vanadium dioxide/pentoxide and the wrapping of these fullerenes in triangular graphene-like envelops. A general theory and review of KrF laser beam interaction with metallorganic liquids are given. A case study of laser beam – V-$(OC_2H_5)_3$ interaction is presented and the subsequent formation steps for graphene, V_2O_5 layers and V_2O_5 fullerenes are outlined.

1.1 Materials that should not exist

More than 70 years ago, Landau and Peierls [1,2] argued that strictly two-dimensional (2D) crystals were thermodynamically unstable and could not exist. Their theory pointed out that a divergent contribution of thermal fluctuations in low-dimensional crystal lattices should lead to such displacements of atoms that they become comparable to inter-atomic distances at any finite temperature. The argument was later extended by Mermin [3] and is strongly supported by a number of experimental observations. Indeed, the melting temperature of thin films rapidly decreases with decreasing thickness, and they become unstable (segregate into islands or decompose) at a thickness of, typically, dozens of atomic layers. For this reason, atomic monolayers have so far been known only as an integral part of larger 3D structures, usually grown epitaxially on top of monocrystals with matching crystal lattices. Without such a 3D base, 2D materials were presumed not to exist until 2004, when the common wisdom was flaunted by the experimental discovery of graphene and other free-

standing 2D atomic crystals (for example, single-layer boron nitride and half-layer BSCCO [4]). These crystals could be obtained on top of non-crystalline substrates, in liquid suspension (Fig. 1) and as suspended membranes. Importantly, the 2D crystals were found not only to be continuous but to exhibit high crystal quality. The latter is most obvious for the case of graphene, in which charge carriers can travel thousands of interatomic distances without scattering. With the benefit of hindsight, the existence of such one-atom-thick crystals can be reconciled with theory. Indeed, it can be argued that the obtained 2D crystallites are quenched in a metastable state because they are extracted from 3D materials, whereas their small size and strong interatomic bonds assure that thermal fluctuations cannot lead to the generation of dislocations or other crystal defects even at elevated temperature.

1.2 What is graphene? Known facts about graphene

Graphene is the name given to a flat monolayer of carbon atoms tightly packed into a two-dimensional (2D) honeycomb lattice, and is a basic building block for graphitic materials of all other dimensionalities (Figure 2). It can be wrapped up into 0D fullerenes, rolled into 1D nanotubes or stacked into 3D graphite.

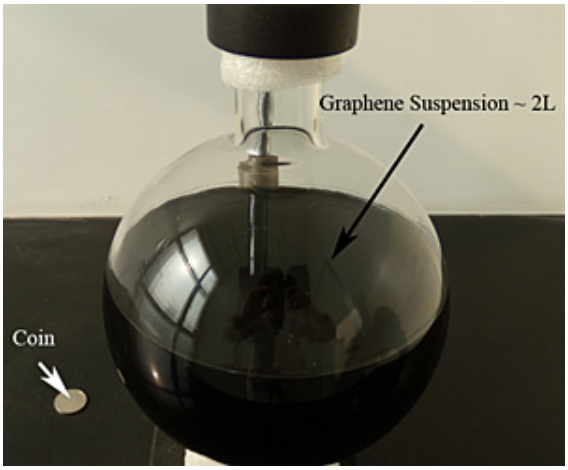

Fig. 1. How graphene suspension looks like

Theoretically, graphene (or "2D graphite") has been studied for sixty years and has been widely used for describing properties of various carbon-based materials. Forty years later, it was realized that graphene also provides an excellent condensed-matter analogue of (2+1)-dimensional quantum electrodynamics, which propelled graphene into a thriving theoretical toy model. On the other hand, although known as integral part of 3D materials, graphene was presumed not to exist in the free state, being described as an "academic" material and believed to be unstable with respect to the formation of curved structures such as soot, fullerenes and nanotubes. All of a sudden, the vintage model turned into reality, when free-standing graphene was unexpectedly found around 2004 by Novoselov and Geim [5] and, especially, when the follow-up experiments confirmed that its charge carriers were indeed massless Dirac fermions [6]. So, the graphene "gold rush" has begun. A complementary viewpoint is that the

extracted 2D crystals become intrinsically stable by gentle crumpling in the third dimension on a lateral scale of ≈10nm. Such 3D warping observed experimentally leads to a gain in elastic energy but suppresses thermal vibrations (anomalously large in 2D), which above a certain temperature can minimize the total free energy.

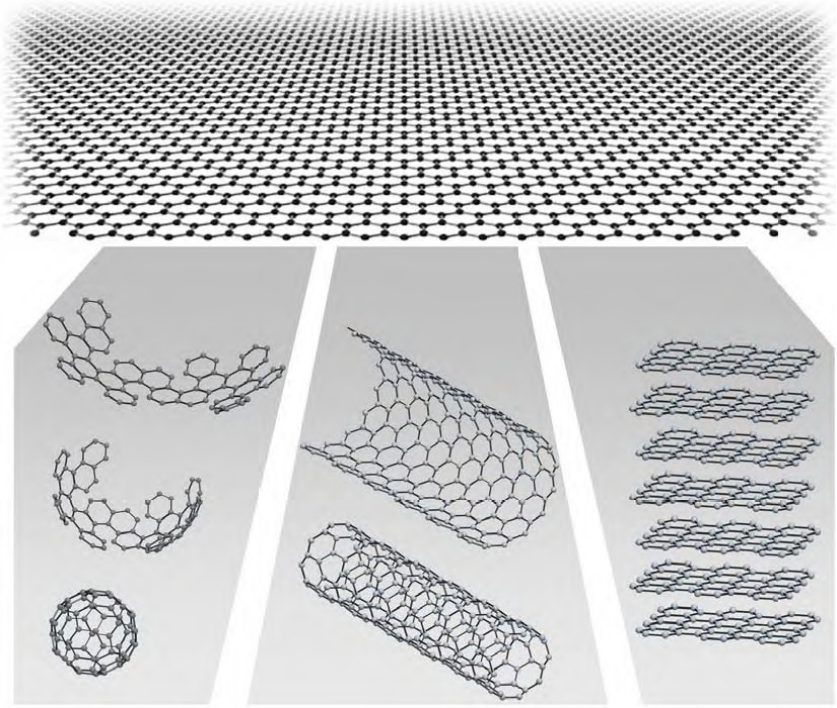

Fig. 2. **Mother of all graphitic forms.** Graphene is a 2D building material for carbon materials of all other dimensionalities. It can be wrapped up into 0D buckyballs, rolled into 1D nanotubes or stacked into 3D graphite [from: Geim and Novoselov, http://arxiv.org/ftp/cond-mat/papers/0702/0702595.pdf]

A single atomic plane *is* a 2D crystal, whereas 100 layers should be considered as a thin film of a 3D material. But how many layers are needed to make a 3D structure? For the case of graphene, the situation has recently become reasonably clear. It was shown that the electronic structure rapidly evolves with the number of layers, approaching the 3D limit of graphite already at 10 layers. Moreover, only graphene and, to a good approximation, its bilayer have simple electronic spectra: they are both zero-gap semiconductors (can also be referred to as zero-overlap semimetals) with one type of electrons and one type of holes. For 3 and more layers, the spectra become increasingly complicated: Several charge carriers appear, and the conduction and valence bands start notably overlapping. This allows one to distinguish between single-, double- and few- (3 to <10) layer graphene as three different types of 2D crystals ("graphenes") [6].

Thicker structures should be considered, to all intents and purposes, as thin films of graphite. From the experimental point of view, such a definition is also sensible. The screening length in

graphite is only ≈5Å (that is, less than 2 layers in thickness) and, hence, one must differentiate between the surface and the bulk even for films as thin as 5 layers. Earlier attempts to isolate graphene concentrated on chemical exfoliation. To this end, bulk graphite was first intercalated (to stage I) so that graphene planes became separated by layers of intervening atoms or molecules. This usually resulted in new 3D materials. However, in certain cases, large molecules could be inserted between atomic planes, providing greater separation such that the resulting compounds could be considered as isolated graphene layers embedded in a 3D matrix. Furthermore, one can often get rid of intercalating molecules in a chemical reaction to obtain a sludge consisting of restacked and scrolled graphene sheets. Because of its uncontrollable character, graphitic sludge has so far attracted only limited interest. There have also been a small number of attempts to grow graphene. The same approach as generally used for growth of carbon nanotubes so far allowed graphite films only thicker than ≈100 layers. On the other hand, single- and few-layer graphene have been grown epitaxially by chemical vapour deposition of hydrocarbons on metal substrates and by thermal decomposition of SiC. Such films were studied by surface science techniques, and their quality and continuity remained unknown. Only lately, few-layer graphene obtained on SiC was characterized with respect to its electronic properties, revealing high-mobility charge carriers. An illustration of a few layers of graphene is given in Figure 3. Epitaxial growth of graphene offers probably the only viable route towards electronic applications and, with so much at stake, a rapid progress in this direction is expected. The approach that seems promising but has not been attempted yet is the use of the previously demonstrated epitaxy on catalytic surfaces (such as Ni or Pt) followed by the deposition of an insulating support on top of graphene and chemical removal of the primary metallic substrate.

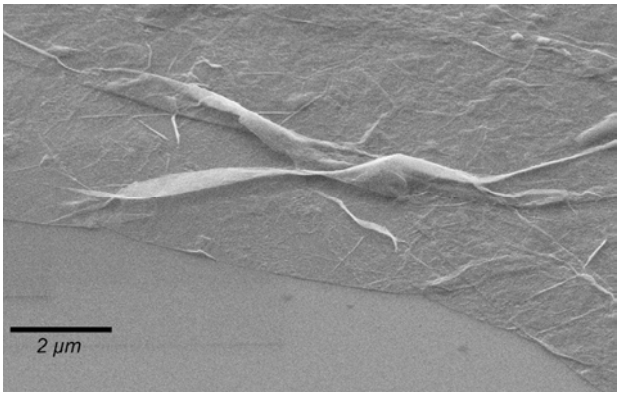

Fig. 3. A few layers of graphene seen by scanning electron microscopy [Taken from www.sineurop-nanotech.com/en/graphene.html Courtsey SINEUROP Nanotech GmbH, Stuttgart, Germany]

1.3 How does one tell if it is graphene? Counting the number of graphene layers

1.3.1 Transmission electron microscopy (TEM)

Transmission electron microscopy is a two-dimensional microscopy technique. It is difficult to probe the third dimension by this technique. The only way to measure the thickness of graphene layers is by performing cross-sectional TEM which can be accomplished by mounting the sample such that the electrons from the gun run parallel to the surface of the graphite layer.

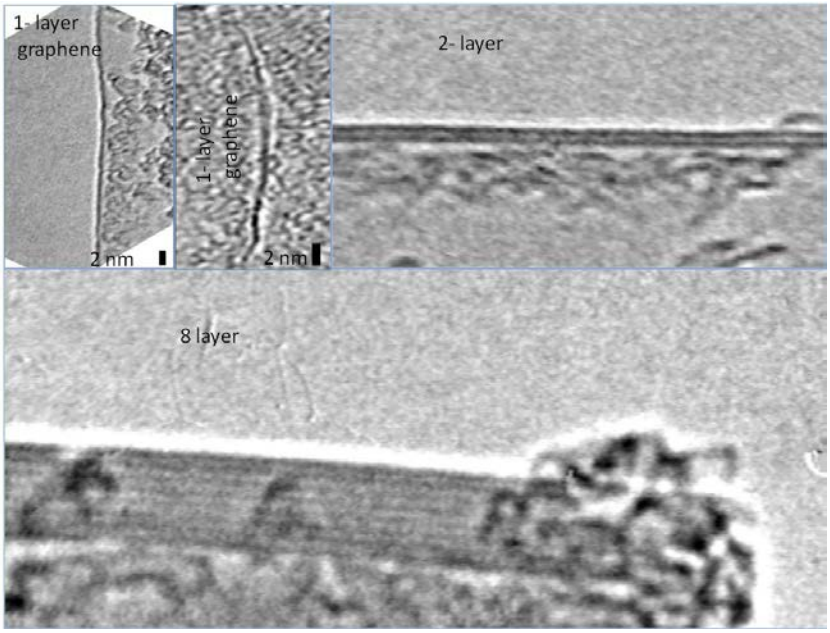

Fig. 4. Counting the number of layers of graphene by high resolution TEM (From A.C. Ferrari et al [7])

Naturally, graphene edges tend to fold and often show wrinkles in the sheet. Close analysis of the fold edge allows for the ability to count the number of layers.

1.3.2 Atomic force microscopy

By atomic force microscopy (AFM) technique, one is able to view the graphene layer in all the three dimensions. From many studies, AFM images for graphene will range from 0.5 nm to 1.5 nm depending on the chemical contrast between the graphene layer and the substrate. For this reason, determination of the thickness of monolayer of graphene by AFM has to be corroborated by other available techniques such as TEM as mentioned already.

1.3.3 Raman spectroscopy

Raman spectroscopy of carbon materials offers a very important versatility in distinguishing the structures carbon displays viz: amorphous carbon (a-C), tetrahedrally amorphous carbon (ta-C), graphite, highly oriented pyrolytic graphite (HOPG), carbon nanotubes, carbon fullerens, diamond and now graphene. Since graphene is but a single layer of graphite, its Raman signature should contain most of the features that are contained in the graphite's Raman signature. However, there two distinct features that stand out in a monolayer graphene that one cannot see in even two-layer graphene: (1) the slight upshift of the G peak by about 5 cm^{-1} and (2) the enhancement of graphite's shoulder peak to second-order D peak (named traditionally as G') to the expense of the main G' peak.

When excitation laser wavelength in the Raman spectrometer is changed from 514 nm to 633 nm, the signatures become slightly noisy without much noticeable change in the phonon wave-numbers as illustrated in Fig 7. Also, the single 2690 cm^{-1} phonon from the one-layer

graphene is replaced by a main phonon at 2710 cm^{-1} with the 2690 cm^{-1} becoming its shoulder in multi-layer graphite

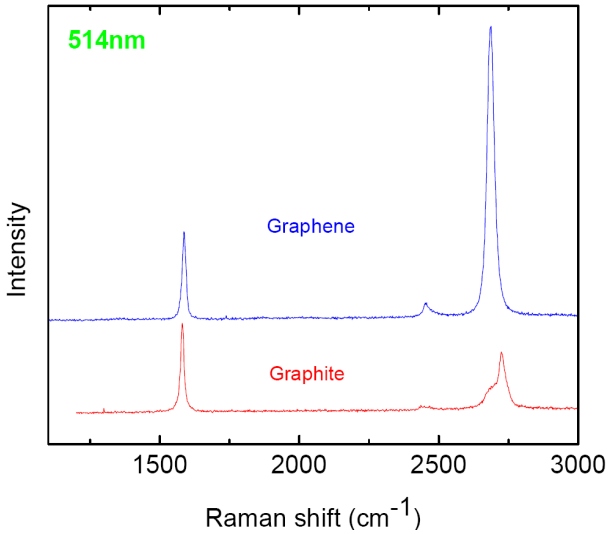

Fig. 5. The Raman signatures for graphene and graphite employing a 514 nm laser wavelength in the Raman spectrometer (From A.C. Ferrari et al [7])

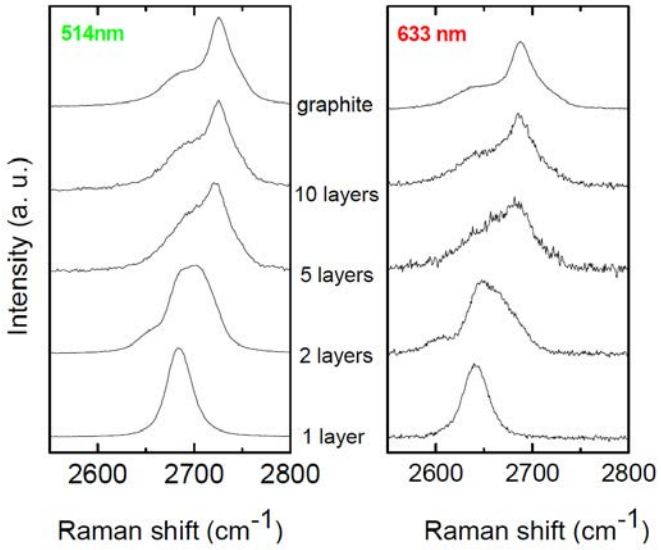

Fig. 6. Raman spectra under 514 nm and 633 nm laser wavelength excitation of the G′ for different number of layers showing the single 2690 cm^{-1} phonon from from the one-layer graphene replaced by a main phonon at 2710 cm^{-1} with the 2690 cm^{-1} becoming its shoulder in multi-layer graphite (From A.C. Ferrari et al [7])

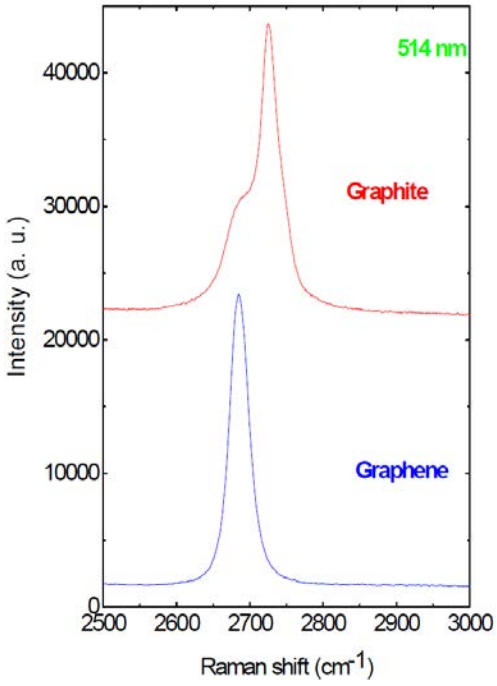

Fig. 7. The single 2690 cm^{-1} phonon from from the one-layer graphene replaced by a main phonon at 2710 cm^{-1} with the 2690 cm^{-1} becoming it shoulder in multi-layer graphite(From A.C. Ferrari et al [7])

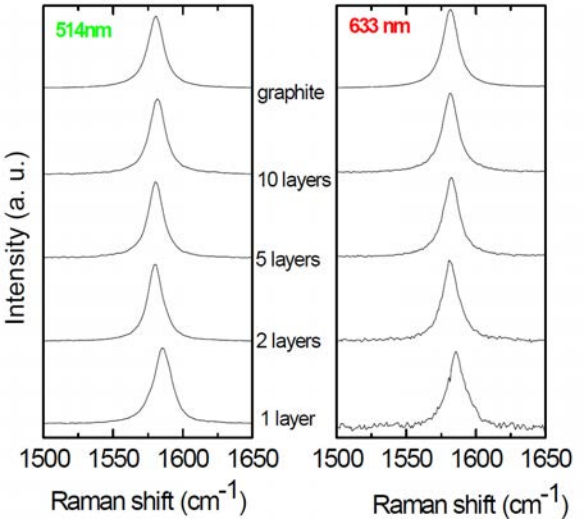

Fig. 8. The slight up-shift of the graphite G peak as the number of grapheme layers decreases to one layer. (From A.C. Ferrari et al [7])

2. Brief review on graphene synthesis

2.1 Top-down versus bottom-up approaches to the realisation of graphene

In a top-down approach, graphene is derived from graphite contained in a pencil lead that we use in everyday life (Figure 9) by stripping layers from a bulk sample. Methods such as the Scotch tape stripping, ion sputtering, pulsed laser deposition, ball milling and arc discharge are all examples of top-down approaches.

Fig. 9. Graphite in a pencil. When writing in pencil you are placing layers of grapheme on paper substrate. Invisible writings could be few layers or even monolayer of graphene. (From A.C. Ferrari et al [7])

Bottom-up routes involve starting at atomic scale and building up atom by atom to the desired final size of the material. Synthesis routes such as chemical vapour deposition (CVD), wet chemistry or the so-called Fischer-Tropsch synthesis, ion implantation, pyrolysis can be regarded as examples of bottom-up approaches. We will review some of these approaches in the sections that follow with regard to the realisation of graphene.

2.2 Chemical vapour deposition

Chemical vapour deposition techniques involve, in general, the decomposition of fluid (gas and liquid sprays) at high temperature to form either thin films on substrates or powders through filters. There are many forms of CVD including: hot wire CVD, thermal CVD, plasma enhanced (PE) CVD, radio-frequency (RF) CVD, ultrasonic spray pyrolysis (USP) among many derivatives. A typical system is illustrated in Figure 10. Graphene synthesis by this method has been reported from around 2008 [8-21], that is, about four years after the discovery of single layer graphene by physical exfoliation. Table 1 summarizes some of the conditions for obtaining single to few layer graphene on various substrates employing the stipulated catalysts in each case. Note that the list is not exhaustive. Before 2000 [19,20], only $C_{14}N$ to $C_{16}N$ (or N doped graphene) layers are reported.

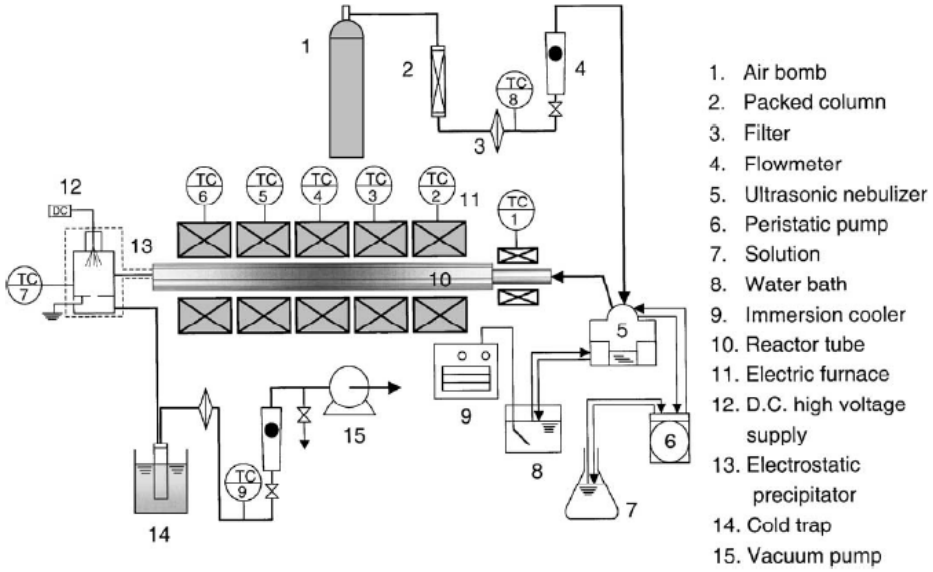

Fig. 10. Schematic illustration of a typical CVD system [From B W Mwakikunga PhD thesis, University of the Witwatersrand (2009)]

Precursor	Temperature	Pressure	Catalyst	Type of CVD	References
Hydrocarbons		Std P	Bi-metallic	RF-CVD	E. Dervishi 2011
Hydrocarbons	900 - 1000 ^{o}C	Std P	c-sapphire, Co/SiO_2 and H_2 (annealing)	Epitaxial CVD	H Ago et al 2010
Methane			Ni and Cu in ammonia		Park et al 2010
Ethylene			Bi-metallic	RF-CVD	E. Dervishi 2010
Methane and H_2	850-1000 ^{o}C		Ni thin film	CVD	Lee et al 2010
Iron tetra-pyridino-porphyrazine				Pyrolysis	Xu et al 2010
methane		Atm, Torr Vacuum	Cu	APCVD LPCVD UHVCVD	Bhaviripudi et al 2010
Methane on HOPG			Fe		Kholmanov 2010
Methane	1000 oC		Co on MgO Argon flow		Wang, X (2009)
Methane	700 oC		Fe	PECVD	Malesevic 2008
Methane	1400-1900 oC		6H SiC	PECVD	Cambaz, Z.G., (2008)

Table 1. A summary of some of the parameters for obtaining graphene by CVD

2.3 Arc discharge

In the arc discharge technique, graphite rods are used as electrodes for high voltage arc-ing. At extremely high voltages between the electrodes that are separated by very small distances, very high electric fields can be produced leading to instantaneous sparks like in a welding process. The fall-out during the discharge process is the end product that contains the carbon nano-structures.

Volotskova et al [22] have reported on deterministic, single-step approach to simultaneous production and magnetic separation of graphene flakes and carbon nanotubes. In this arc discharge process, by employing magnetic fields, nanotubes and graphene are deposited in different areas. These results are very relevant to the development of commercially-viable, single-step production of bulk amounts of high-quality graphene. Also Li et al [23] have reported the existence of double layered graphene sheets in their arc discharge "debris".

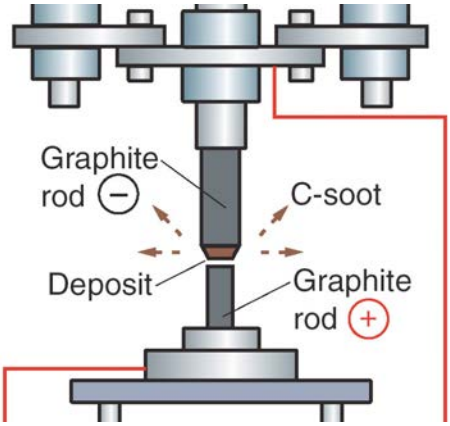

Fig. 11. A typical arc discharge system [mrsec.wisc.edu/.../images/nanotubes/arc.jpg]

2.4 Fischer-Tropsch synthesis

The Fischer–Tropsch process (or Fischer–Tropsch Synthesis) is a set of chemical reactions that convert a mixture of carbon monoxide and hydrogen into liquid hydrocarbons. The process, a key component of gas to liquids technology, produces a petroleum substitute, typically from coal, natural gas, or biomass for use as synthetic lubrication oil and as synthetic fuel. The F-T process has received intermittent attention as a source of low-sulfur diesel fuel and to address the supply or cost of petroleum-derived hydrocarbons.

The Fischer–Tropsch process involves a series of chemical reactions that lead to a variety of hydrocarbons. Useful reactions give alkanes, $(2n+1)H_2 + nCO \rightarrow C_nH_{(2n+2)} + nH_2O$, where n is a positive integer. The formation of methane (n = 1) is generally unwanted. Most of the alkanes produced tend to be straight-chain alkanes, although some branched alkanes are also formed. In addition to alkane formation, competing reactions result in the formation of alkenes, as well as alcohols and other oxygenated hydrocarbons. Usually, only relatively small quantities of these non-alkane products are formed, although catalysts favoring some of these products have been developed.

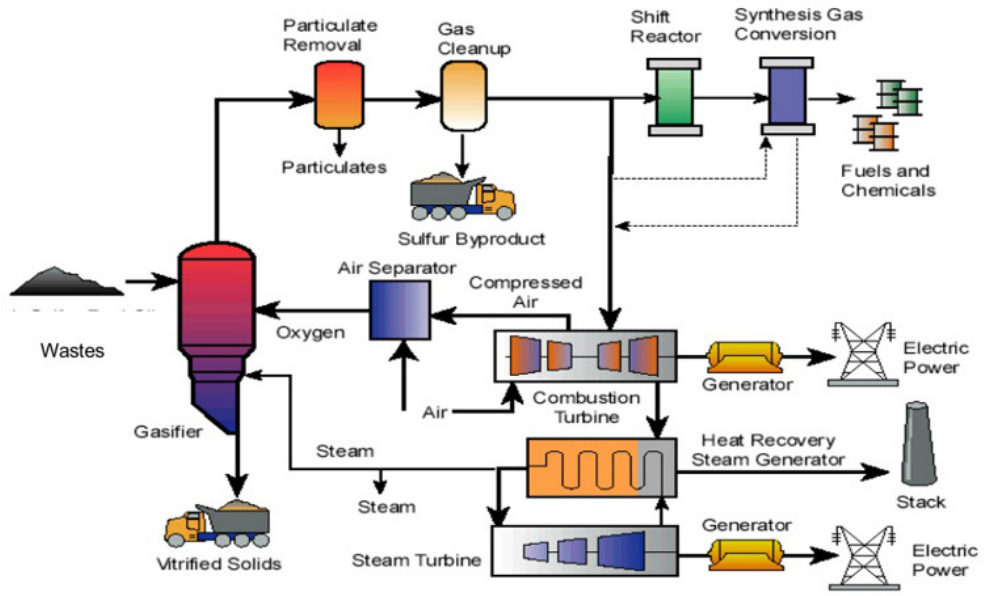

Fig. 12. An illustration of the Fischer-Tropsch synthesis [www.rccostello.com/copure.html]

Recently [24], Fischer-Tropsch Synthesis (FTS) reactions have suggested possibility to obtain carbon and H_2O rather than alkanes and H_2O through the reaction $(2n+1)H_2 + nCO \rightarrow C$ (graphene) + nH_2O when the catalysis and other parameters are varied. For instance, the deactivation of a 20 wt% $Co/\gamma\text{-}Al_2O_3$ catalyst during the FTS at 240 °C, 20 bar, and a H_2:CO ratio of 2 was studied in a fixed-bed micro-reactor [Fei]. The CO conversion had reduced by 30% after 200 h, and both carbidic and polyaromatic carbon species could be detected on the catalyst using a combination of Temperature-Programmed Hydrogenation (TPH), X-ray Photoelectron Spectroscopy (XPS) and High Resolution Transmission Electron Microscopy (HRTEM). Using Density Functional Theory (DFT), the relative stability of different types of deposited carbon on the Co catalyst was evaluated. Extended layers of graphene were the most stable form, followed by a p4g surface carbide phase initiating from the step edges. Both are more stable than surface CH_2 groups by 99 and 79 kJ/mol.

Also Swart et al [25] have studied the possible catalyst deactivation mechanisms in the FTS synthesis of graphene overlayer by elucidating the adsorption of graphene on the fcc – Co(111) surface. A chemical interaction between the graphene sheet and the cobalt surface was observed as evidenced by the partial DOS and Bader charge analysis. The adsorption energy was found to be small when normalized per carbon atom, but becoming large for extended graphene sheets. Graphene removal from the surface via lifting or sliding was considered. The energy barrier for sliding a graphene sheet is lower than the barrier for lifting, but the energy barriers become significant when placed into the context of realistic catalytic surfaces in the nano-meter range.

Also Nolan et al [26] have deposited graphene on metal catalysts by this method. Carbon formed from CO in CO_2 at around 500°C deposited as nanotubes and encapsulating carbons on a supported Ni catalyst without H_2 or as filaments if H_2 was present. By a thermodynamic model, they explained how hydrogen in low concentrations controls filament morphology and why equilibrium is shifted from that for graphite during carbon deposition. Carbon deposition reaction rates at low carbon activity in the absence of hydrogen were reported. When hydrogen was present, a series of hydrocarbons formed, as in fuel synthesis (Fischer-Tropsch) chemistry. Surface vinyl species that have been recently shown to be intermediates in Fischer-Tropsch chemistry also polymerized to form graphene. The formation of vinyls from CO and H via surface alkyls occurred at a greater rate than methane formation when the supply of hydrogen was limited. Hydrogen from the bulk catalyst metal (not surface adsorbed) hydrogenates the surface alkyls, indicating that hydrogen solubility may control the metal-catalyzed formation of various hydrocarbons and eventually solid graphitic carbon.

2.4 High Temperature High Pressure technique

Graphene has been produced by a high pressure-high temperature (HPHT) growth process from the natural graphitic source material by utilising the molten Fe-Ni catalysts for dissolution of carbon [27]. The method may lead to a more reliable graphene synthesis and facilitate its purification and chemical doping.

2.5 Sputtering

During the co-sputtering of C and Cu into a carbon matrix [28], a demixing (segregation) occurs of the carbon and copper species due to their very low solubilities that leads to the formation of nanometric copper precipitates homogeneously distributed in a more or less graphitic matrix. These precipitates have an elongated shape in the direction of the thin film growth. When the deposition was performed at 273 K for copper atomic concentrations $C_{Cu} > 55\%$, as well as for all thin films synthesized at 573 K whatever the C_{Cu} value, the formation of graphene layers parallel to the surface of the copper precipitates was observed so that an encapsulation of the Cu aggregates in carbon cages occurs.

2.6 Wet chemistry and sonication

Graphene-like carbon sheets can be synthesized, for instance, from adamantane in the solution phase at ambient temperature. Adamantane, $C_{10}H_{16}$, has a tetracyclic ring structure with four cyclohexanes in chair conformation. The two dimensional carbon structures have been obtained by introducing ferrocene as the catalyst precursor and adamantane as the carbon source under sonication [29], proving that cyclohexane structures in adamantane can serve as a building block for graphene formation. The synthesized carbon sheets were characterized and confirmed by X-ray diffraction, high-resolution electron microscopy and atomic force microscopy.

Also, nanostructured CN_x thin films were prepared by supersonic cluster beam deposition (SCBD) [30]. Films containing bundles of well-ordered graphene multilayers, onions and nanotubes embedded in an amorphous matrix were grown alongside purely amorphous films by changing the deposition parameters. Graphitic nanostructures were synthesized without using metallic catalysts.

2.7 Unzipping of SWCNT into monolayer graphene

A very ingenious idea on realising a monolayer graphene by unzipping single wall carbon nanotubes has been reported recently [31]. At this scale, the unzipping, has been accomplished by harsh acids and the right thermodynamic conditions. A computer generated illustration of the unzipping process is illustrated in Figure 12.

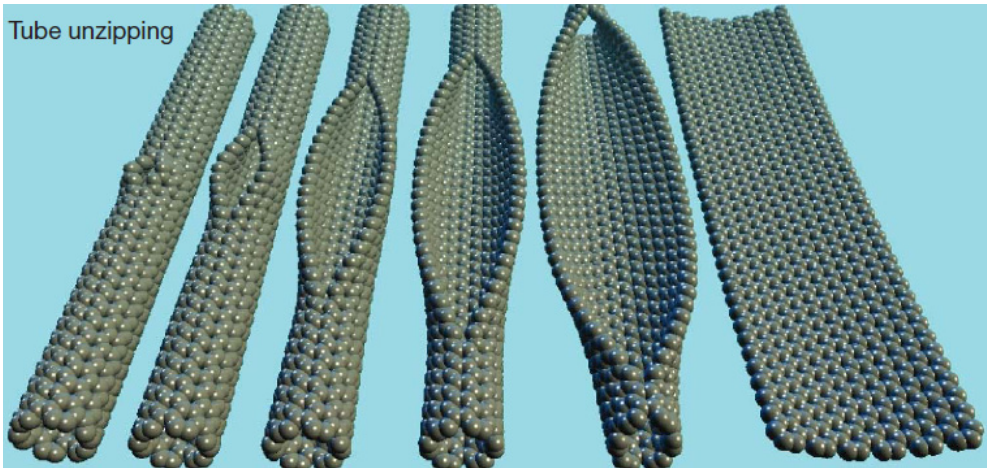

Fig. 12. Modelling illustration of the SWCNT unzipped into monolayer graphene [31]

2.8 Carbon implantation into catalyst substrates

Ion implantation method for large-scale synthesis of high quality graphene films with controllable thickness has been demonstrated [32,33]. Thermally annealing polycrystalline nickel substrates that have been ion implanted with carbon atoms results in the surface growth of graphene films whose average thickness is controlled by implantation dose. The implantation synthesis method can be generalized to a variety of metallic substrates and growth temperatures, since it does not require a decomposition of chemical precursors or a solvation of carbon into the substrate.

3. Graphene by laser solution photolysis

Laser synthesis methods have been of particular interest [34, 35]. The coherent, intense and almost monochromatic laser light allows it to be tuned to selectively dissociate specific bonds in a precursor molecule either by resonance between the laser frequency and the bond's natural frequency or via multi-photon absorption. This leads to products that can be unique and different from those obtained by traditional thermal deposition techniques. In this work, we followed a process called laser solution photolysis (LSP) that has been used previously to obtain FePt ultra-fine powders [36]. Organo-metallic

precursors containing Fe and Pt, respectively were employed in the presence of a polymer. The polymer was employed to reduce agglomeration of the nano-particles produced. Further examples of the technique include, gold nanoparticles produced by UV light irradiation of gold chloride [37–39], iron-based nanoparticles produced by utilising UV light absorbing ferrocene and iron(II) acetylacetonate [40, 41] and laser ablation in a solid– liquid interface [42, 43].

In a study where metal ethoxide precursors, which were produced from metal chlorides reacted with ethanol, were employed in conjunction with the KrF laser at a wavelength of 248 nm to produced not only quantum dots but also graphene layers.

Triangular envelope-like structures of about 400 nm on each side of the triangle are the predominant polymorphs. The triangles are thin layers of VO_x with an interplanar spacing of 3.75 Å as shown in Fig. 13. Observed at higher magnification, the layers were found to be envelopes containing spherical nano-particles with an average size of 6 nm. These VO_x quantum dots which can be solid (multi-walled) spheres or VO_x fullerenes are found to have the same size distribution.

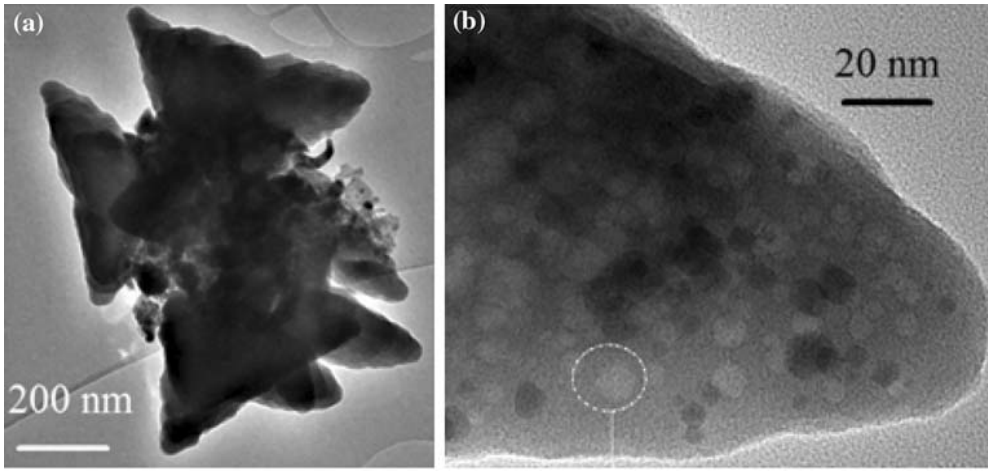

Fig. 13. (a) Low magnification TEM of the triangular envelopes of VO_x, (b) one pocket at higher magnification, showing the small voids and solid spheres. The spheres have been found to be inorganic fullerenes of VO_x segregated from graphene sheet that forms the envelope [52].

The strong and broad absorption peak at 598 cm^{-1} with its shoulder at 730 cm^{-1} can be assigned to the O–W–O stretching vibrations in the WO3 structure, whereas the 916 cm^{-1} peak corresponds to the W=O surface stretching modes due to dangling oxygen bonds. The red-shift from the Raman allowed 960 cm^{-1} to the IR allowed 916 cm^{-1} could be due to the loading of carbon on these bonds. Carbon doping is confirmed by the presence of the peaks assigned to the C–O bonding at 1,000 and 1,054 cm^{-1}; these could not be observed in Raman

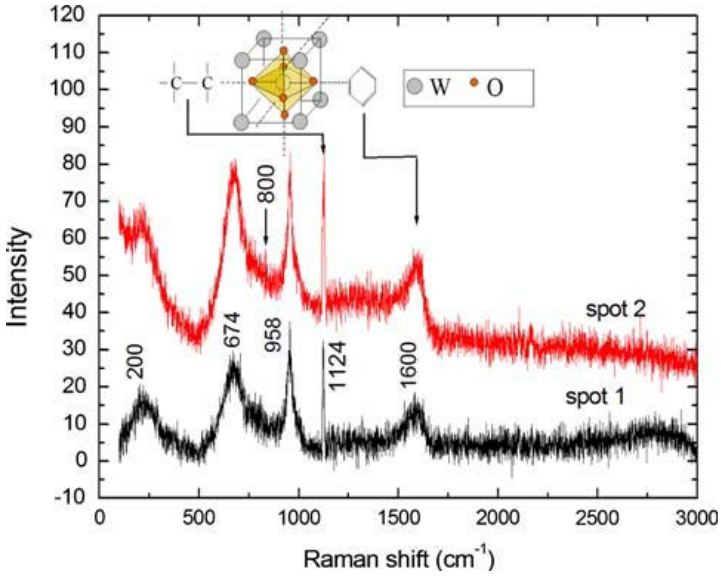

Fig. 14. Raman spectra of metal oxide QD-functionalised graphene. The G peak at 1600 cm^{-1} and the G′ at 2700 cm^{-1} on spot 1 are signatures from graphene layers. The rest of the peaks are from the metal oxides (VO_2 and WO_3) [52]

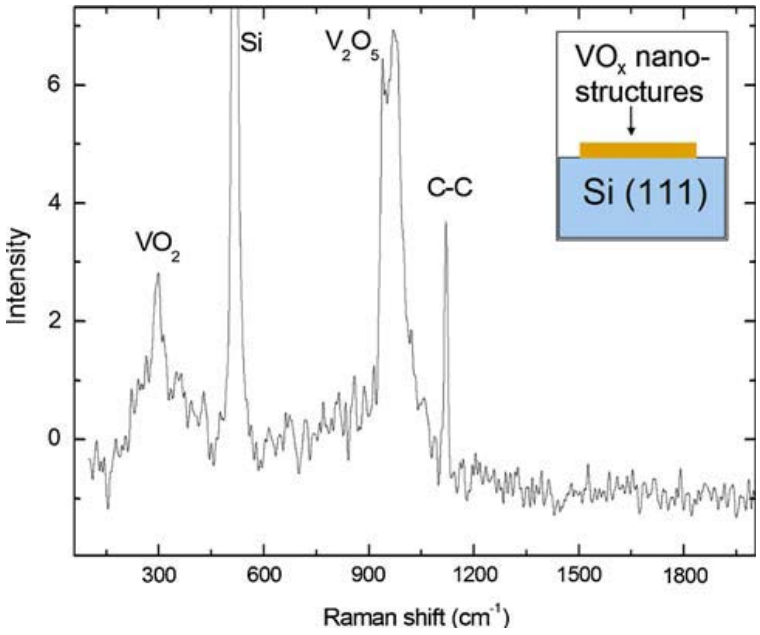

Fig. 15. Raman spectrum of inorganic fullerenes of VO_x nanostructures [52]

spectroscopy for reasons not established yet. The 1,600 cm^{-1} phonon frequency assigned to the perfect graphite's aromatic carbon ring is confirmed by FTIR as previously seen in Raman spectroscopy. The group of absorption peaks from 3,000 to 3,550 cm^{-1} have previously been assigned to OH bonds which suggest that some terminal oxygen atoms in the WO_3 structure are not only bonded to the carbon aromatic rings but also to hydrogen. No C–H bonds were found by FTIR.

Raman spectroscopy of these structures supports the fact that there exists mixed valence of V^{4+} (signified by the 300 cm^{-1} phonon which is an undertone of the main 600 cm^{-1} peak which in these samples is masked by the strong Si–Si background noise from the substrate at 520 cm^{-1}) and V^{5+} from 930–970 cm^{-1}. The peak at 1,120 cm^{-1} suggests the presence of C–C bonds in the VO_2/V_2O_5 structure. As opposed to the carbon modified WO_3 nano-platelets which showed aromatic carbon apart from C–C bonds, Raman spectroscopy showed no aromatic rings in VO_2/V_2O_5 triangular envelopes.

4. Possible mechanism of formation of the triangular envelopes made out of graphene sheets and VO_x inorganic fullerenes

Since the discovery of carbon nano-tube structure in the early 1980s, Tenne and co-workers also reported similar structures in WSe_2 and MoS_2 [46]. The argument was that metal chalcogenides and oxides are also capable of arranging their unit cells in a hexagonal close packing as in carbon, thereby forming a layer of atoms whose edges leave dangling bonds. These bonds cause intense attractive forces which compel the layer to fold on itself into various shapes such as tubes, scrolls and rods. Formation of fullerenes is due to defects which are found to be pentagonal, rectangular and triangular bonds, which are possible in all transition metal compounds. Different processes of formation of, for instance, V_2O_5 capsules [47, 48] have led authors to suggest various mechanisms. We suggest that the formation of our triangular envelopes/capsules starts with the formation of closely packed hexagonal 2-D layers when the VO_x is subjected to the laser beam. This assumption is based on the known experimental and theoretical facts from computer modelling that V_2O_5 is capable of wrapping into V_2O_5 nano-tubes [49] either as a zig–zag framework or in an arm chair structure [50]. It is also known that a mixture of V^{4+} and V^{5+} in $(V^{IV}O)[V^{V}O_4]_{.0.5}[C_3N_2H_{12}]$ can lead to a layered structure [51]. The organic layer intercalates the inorganic counterpart with the latter containing square pyramids formed by V^{4+} ions and tetrahedral pyramids formed by V^{5+} ions. On this layer are randomly scattered fullerenes of the same material which have self-assembled under the same laser beam. These fullerenes together with dangling bonds on the layer periphery exert intense attractive forces which cause the layer to fold on itself in a certain pattern. A schematic cartoon of the possible formation of the VO_2/V_2O_5 triangular envelops that encapsulate the VO_2/V_2O_5 QDs and the VO_2/V_2O_5 fullerenes are shown in Fig. 7. A hexagonal packing in a zig–zag fashion ends up having arm-chair structure dangling bonds in the periphery of the hexagon. The dangling bonds and the van der Waal's forces from the particles sitting on the surface compel this sheeting to wrap on itself from a hexagon, through intermediate stages, into a triangular envelope. The foldings are along arm-chair structure on two sides of the triangle AEC (sides AC and EC in Fig. 16 (a)) and along a zig–zag structure on the third side of the triangle (side AE).

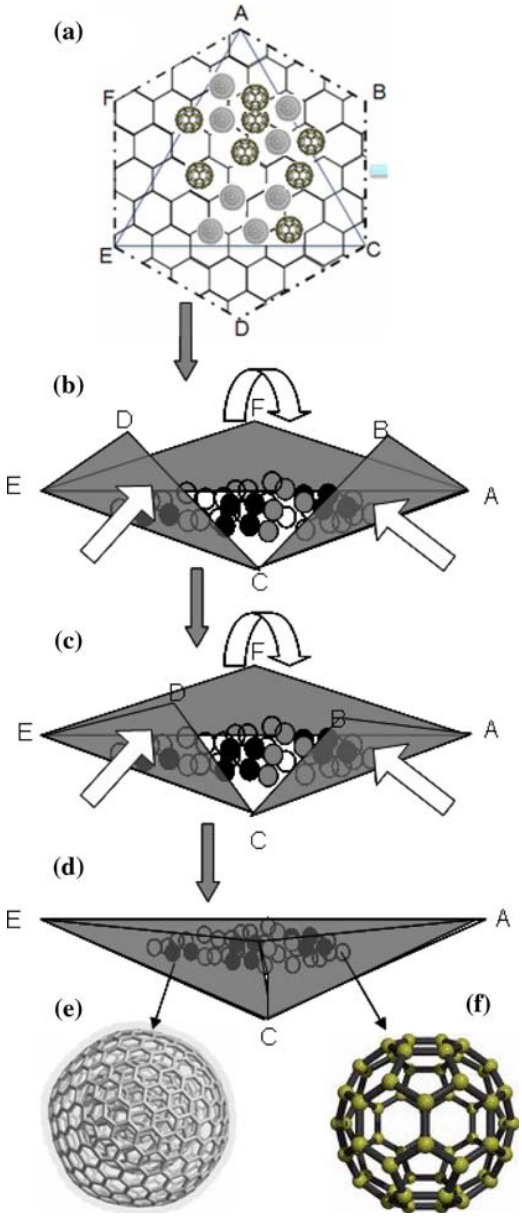

Fig. 16. A schematic representation of how the triangular envelops of graphene sheets as well as VOx sheets form (a) a hexagonally packed layer of V2O5/VO2 with some QDs of same material scattered randomly on it (b) the layer folds along zigzag AE, armchair EC and armchair AC of triangle AEC (c) the folding of triangular flaps ABC, CDE and EDF progresses until (d) the triangular envelop AEC is formed. The enveloped spherical particles are either (e) multi-walled V_2O_5/VO_2 fullerenes or (f) single walled V_2O_5/VO_2 fullerenes [52]

5. Conclusion

We have presented the known facts about graphene and shown the identification methods by Raman spectroscopy and TEM. We have also presented a review of the most recent efforts to move away from the Scotch tape techniques (first discovered by Geim and Novoselov in 2004) to large scale routes towards the synthesis of graphene. We have shown how graphene and graphene-like layers are produced in laser solution photolysis of organo-metallic solutions and how both the inorganic fullerenes and graphene layers are produced and interact with each other. A mechanism for the wrapping of such particles by a graphene sheet is also discussed.

6. References

[1] Peierls, R. E. Quelques proprietes typiques des corpses solides. Ann. I. H. Poincare 5, 177-222 (1935).

[2] Landau, L. D. Zur Theorie der phasenumwandlungen II. Phys. Z. Sowjetunion, 11, 26-35 (1937).

[3] Mermin, N. D. Crystalline order in two dimensions. Phys. Rev. 176, 250-254 (1968)

[4] Novoselov, K. S. et al. Two-dimensional atomic crystals. Proc. Natl Acad. Sci. USA 102, 10451-10453 (2005)

[5] Novoselov, K. S. et al. Electric field effect in atomically thin carbon films. Science 306, 666-669 (2004).

[6] Novoselov, K. S. et al. Two-dimensional gas of massless Dirac fermions in graphene. Nature 438, 197-200 (2005).

[7] A. C. Ferrari,1,* J. C. Meyer,2 V. Scardaci,1 C. Casiraghi,1 M. Lazzeri,3 F. Mauri,3 S. Piscanec,1 D. Jiang,4, K. S. Novoselov,4 S. Roth,2 and A. K. Geim4, Raman Spectrum of Graphene and Graphene Layers, Phys. Rev. Lett. 97, 187401 (2006)

[8] Dervishi, E., Li, Z., Shyaka, J., Watanabe, F., Biswas, A., Umwungeri, J.L., Courte, A., Biris, A.S., The role of hydrocarbon concentration on the synthesis of large area few to multi-layer graphene structures, Chemical Physics Letters 501 (4-6), 390-395 (2011)

[9] Ago, H., Ito, Y., Mizuta, N., Yoshida, K., Hu, B., Orofeo, C.M., Tsuji, M., Mizuno, S., Epitaxial chemical vapor deposition growth of single-layer graphene over cobalt film crystallized on sapphire, ACS Nano 4 (12), 7407-7414 (2010)

[10] Park, H.J., Skákalová, V., Meyer, J., Lee, D.S., Iwasaki, T., Bumby, C., Kaiser, U., Roth, S., Growth and properties of chemically modified grapheme, Physica Status Solidi (B) Basic Research 247 (11-12), pp. 2915-2919 (2010)

[11] Dervishi, E., Li, Z., Shyaka, J., Watanabe, F., Biswas, A., Umwungeri, J.L., Courte, A., Biris, A.S., Large area graphene sheets synthesized on a bi-metallic catalyst system, Nanotechnology 2010: Advanced Materials, CNTs, Particles, Films and Composites - Technical Proceedings of the 2010 NSTI Nanotechnology Conference and Expo, NSTI-Nanotech 2010 1, 234-237 (2010)

[12] Lee, B.-J., Yu, H.-Y., Jeong, G.-H., Controlled synthesis of monolayer graphene toward transparent flexible conductive film application, Nanoscale Research Letters 5 (11), 1768-1773 (2010)

[13] Xu, Z., Li, H., Cao, G., Cao, Z., Zhang, Q., Li, K., Hou, X., (...), Cao, W. Synthesis of hybrid graphene carbon-coated nanocatalysts, Journal of Materials Chemistry 20 (38), pp. 8230-8232 (2010)

[14] Bhaviripudi, S., Jia, X., Dresselhaus, M.S., Kong, J., Role of kinetic factors in chemical vapor deposition synthesis of uniform large area graphene using copper catalyst, Nano Letters 10 (10), pp. 4128-4133 (2010)

[15] Kholmanov, I.N., Cavaliere, E., Cepek, C., Gavioli, L., Catalytic chemical vapor deposition of methane on graphite to produce graphene structures, Carbon 48 (5), pp. 1619-1625 (2010)

[16] Wang, X., You, H., Liu, F., Li, M., Wan, L., Li, S., Li, Q., (...), Cheng, J., Large-scale synthesis of few-layered graphene using CVD, Chemical Vapor Deposition 15 (1-3), 53-56 (2009)

[17] Malesevic, A., Vitchev, R., Schouteden, K., Volodin, A., Zhang, L., Tendeloo, G.V., Vanhulsel, A., Haesendonck, C.V., Synthesis of few-layer graphene via microwave plasma-enhanced chemical vapour deposition, Nanotechnology 19 (30), art. no. 305604 (2008)

[18] Cambaz, Z.G., Yushin, G., Osswald, S., Mochalin, V., Gogotsi, Y., Noncatalytic synthesis of carbon nanotubes, graphene and graphite on SiC, Carbon 46 (6), pp. 841-849 (2008)

[19] Nakajima, T., Koh, M., Takashima, M., Electrochemical behavior of carbon alloy CxN prepared by CVD using a nickel catalyst, Electrochimica Acta 43 (8), 883-891 (1997)

[20] Nakajima, T., Koh, M., Synthesis of high crystalline carbon-nitrogen layered compounds by CVD using nickel and cobalt catalysts, Carbon 35 (2), pp. 203-208 (1997)

[21] Rümmeli, M.H., Kramberger, C., Grüneis, A., Ayala, P., Gemming, T., Büchner, B., Pichler, T., On the graphitization nature of oxides for the formation of carbon nanostructures, Chemistry of Materials 19 (17), 4105-4107 (2007)

[22] Volotskova, O., Levchenko, I., Shashurin, A., Raitses, Y., Ostrikov, K., Keidar, M., Single-step synthesis and magnetic separation of graphene and carbon nanotubes in arc discharge plasmas, Nanoscale 2 (10), 2281-2285 (2010)

[23] Li, B.-J., Kung, S.-C., Hsu, C.-M., Gao, J.-Y., Lai, H.-J., Preparation of a new carbon nano-partlcle by arc discharge, Materials Research Society Symposium Proceedings 822, art. no. S6.12, pp. 115-120 (2004)

[24] Fei Tan, K., Xu, J., Chang, J., Borgna, A., Saeys, M., Carbon deposition on Co catalysts during Fischer-Tropsch synthesis: A computational and experimental study, Journal of Catalysis 274 (2), 121-129 (2010)

[25] Swart, J.C.W., Van Steen, E., Ciobíč, I.M., Van Santen, R.A., Interaction of graphene with FCC-Co(111), Physical Chemistry Chemical Physics 11 (5), pp. 803-807 (2009)

[26] Nolan, P.E., Lynch, D.C., Cutler, A.H., Carbon deposition and hydrocarbon formation on group VIII metal catalysts, Journal of Physical Chemistry B 102 (21), 4165-4175 (1998)

[27] Parvizi, F., Teweldebrhan, D., Ghosh, S., Calizo, I., Balandin, A.A., Zhu, H., Abbaschian, R. Cabioc'h, T., Naudon, A., Jaouen, M., Thiaudiére, D., Babonneau, D., Co-sputtering C - Cu thin film synthesis: Microstructural study of copper precipitates encapsulated into a carbon matrix, Philosophical Magazine B: Physics of Condensed Matter; Statistical Mechanics, Electronic, Optical and Magnetic Properties 79 (3), pp. 501-516 (1999)

[28] Jee, A.-Y., Lee, M., Synthesis of two dimensional carbon sheets from adamantane, Carbon 47 (10), 2546-2548 (2009)

[29] Bongiorno, G., Blomqvist, M., Piseri, P., Milani, P., Lenardi, C., Ducati, C., Caruso, T., Coronel, E., Nanostructured CNx (0 < x < 0.2) films grown by supersonic cluster beam deposition, Carbon 43 (7) 1460-1469 (2005)
[30] Dmitry V. Kosynkin, Amanda L. Higginbotham, Alexander Sinitskii, Jay R. Lomeda, Ayrat Dimiev, B. Katherine Price, James M. Tour, Longitudinal unzipping of carbon nanotubes to form graphene nanoribbons, Nature 458, 872 (2009)
[31] Laurent Baraton, Zhanbing He, Chang Seok Lee, Jean-Luc Maurice, Costel Sorin Cojocaru, Anne-Franc¸oise Gourgues-Lorenzon, Young Hee Lee and Didier Pribat, Synthesis of few-layered graphene by ion implantation of carbon in nickel thin films, Nanotechnology 22 (2011) 085601 (5pp)
[32] Slaven Garaj, William Hubbard, and J. A. Golovchenko, Graphene synthesis by ion implantation, Appl. Phys. Lett. 97, 183103 (2010)
[33] B.W. Mwakikunga, A. Forbes, E. Sideras-Haddad, R.M. Erasmus, G. Katumba, B. Masina, Int. J. Nanoparticles 1, 3 (2008)
[34] B.W. Mwakikunga, A. Forbes, E. Sideras-Haddad, C. Arendse, Nanoscale Res. Lett. 3, 372 (2008)
[35] M. Watanabe, H. Takamura, H. Sugai, Nanoscale Res. Lett. 4, 565 (2009)
[36] H. Hada, Y. Yonezawa, A. Yoshida, A. Kurakake, J. Phys. Chem. 80, 2728 (1976)
[37] K. Kurihara, J. Kizling, P. Stenius, J.H. Fendler, J. Am. Chem.Soc. 105, 2574 (1983)
[38] L. Bronstein, D. Chernshov, P. Valetsky, N. Tkachenko, H. Lemmetyinen, J. Hartmann, S. Forster, Langmuir 15, 83 (1999)
[39] J.A. Powell, S.R. Logan, J. Photochem. 3, 189 (1974)
[40] J. Pola, M. Marysko, V. Vorlicek, S. Bakardjieva, J. Subrt, Z. Bastl, A. Ouchi, J. Photochem. Photobiol. Chem. 199, 156 (2008)
[41] C. Liang, Y. Shimizu, M. Masuda, T. Sasaki, N. Koshizaki, Chem. Mater. 16, 963 (2004)
[42] Y. Ishikawa, K. Kawaguchi, Y. Shimizu, T. Sasaki, N. Koshizaki, Chem. Phys. Lett. 428, 426 (2006)
[43] J. Livage, Chem. Mater. 3, 578 (1991)
[44] A. Picard, I. Daniel, G. Montagnac, P. Oger, Extremophiles 11, 445 (2007)
[45] A.C. Ferrari, J. Robertson, Phys. Rev. B 64, 075414 (2001)
[46] R. Tenne, I. Margulis, M. Genut, G. Hodes, Nature 360, 444 (1992)
[47] J. Liu, D. Xue, Adv. Mater. 20, 2622 (2008)
[48] J. Liu, F. Liu, K. Gao, J. Wu, D. Xue, J. Mater. Chem. 19, 6073 (2009)
[49] G.T. Chandrappa, N. Stenou, S. Cassaignon, C. Bauvis, J. Livage, Catal. Today 78, 85 (2003)
[50] V.V. Ivanovskaya, A.N. Enyashin, A.A. Sofronov, Y.N. Makurin, N.I. Medvedeva, A.L. Ivanovskii, Solid State Commun. 126, 489 (2003)
[51] D. Riou, G. Ferey, J. Solid State Chem. 120, 137 (1995)
[52] B. W. Mwakikunga, A. Forbes, E. Sideras-Haddad, M. Scriba, E. Manikandan, Self Assembly and Properties of C:WO3 Nano-Platelets and C:VO2/V2O5 Triangular Capsules Produced by Laser Solution Photolysis, Nanoscale Res Lett. 5, 389 (2010)